Strain accommodation in inelastic deformation of glasses

P. Murali,[1] U. Ramamurty,[1] and Vijay B. Shenoy[2,3,*]
[1]*Department of Materials Engineering, Indian Institute of Science, Bangalore 560012, India*
[2]*Materials Research Centre, Indian Institute of Science, Bangalore 560012, India*
[3]*Centre for Condensed Matter Theory, Indian Institute of Science, Bangalore 560012, India*
(Received 3 June 2006; revised manuscript received 17 October 2006; published 5 January 2007)

Motivated by recent experiments on metallic glasses, we examine the micromechanisms of strain accommodation including crystallization and void formation during inelastic deformation of glasses by employing molecular statics simulations. Our atomistic simulations with Lennard-Jones-like potentials suggests that a softer short range interaction between atoms favors crystallization. Compressive hydrostatic strain in the presence of a shear strain promotes crystallization whereas a tensile hydrostatic strain is found to induce voids. The deformation subsequent to the onset of crystallization includes partial reamorphization and recrystallization, suggesting important atomistic mechanisms of plastic dissipation in glasses.

DOI: 10.1103/PhysRevB.75.024203 PACS number(s): 62.20.Fe, 61.43.Fs, 61.82.Rx, 02.70.Ns

I. INTRODUCTION

Plastic flow in metallic glasses at high strain rates and low temperatures occurs by shear localization into narrow bands, referred to as shear bands. While several experiments have been conducted to understand the micromechanisms of plasticity in metallic glasses, precise understanding of the atomic processes involved in the shear band formation and propagation is far from complete. In particular, recent experiments suggest the possibility of deformation-induced crystallization as well as nano-void formation.[1–6] Chen *et al.*,[1] first reported deformation-induced crystallization during bending of metallic glass ribbon samples and attributed it to the localized melting due to adiabatic heating in the shear bands. The relatively slow cooling that follows deformation induces crystallization in these materials. Kim *et al.*[2] performed quasistatic nanoindentation and observed nanocrystallites in the shear bands which rules out the possibility of localized melting. They argue that flow-induced dilatation of disordered structures enhances diffusional activity which aids in crystallization; this is in contradiction to Chen's hypothesis. Further complexity is added to this by the high resolution electron microscopic observations of Hufnagel *et al.*,[3] who report the observation of nano-voids in shear bands. Jiang and Atzmon[4] suggest that whether nanocrystallization or nano-voids form in shear bands depend on the state of stress—tension favors nano-voids whereas compression leads to nanocrystallization. Bhowmick *et al.*,[5] show that nano-void formation leads to strain softening in metallic glasses. Recently, Lee *et al.*[6] examined the crystallization-induced plasticity and observed that compressive loading and low activation energy for the crystallization process as the governing parameters for plasticity in amorphous alloys. Molecular dynamics simulations have been performed by Tarumi *et al.*[7] using morse pair potentials and Lee *et al.*[8] using the modified embedded atom method (MEAM) potentials, both reporting deformation induced crystallization in amorphous materials.

It has been established from several experiments that metallic glasses exhibit asymmetry in tension and compression and their yield criteria are normal-stress dependent.[9–11] Lund and Schuh[12] performed molecular statics simulations on unit atomic clusters (or shear tansformation zones) to show that macroscopic yield criteria of an amorphous system follows Mohr-Coulumb law. Therefore it is reasonable to expect atomic processes in shear bands to be influenced by the stress state. This work is undertaken with the objective of understanding what controls the micromechanisms such as crystallization and void formation during the inelastic deformation of glasses. Clearly, the nature of atomic interactions and the state of stress determine which micromechanism operates. Here we perform molecular simulations to study both these factors viz. the influence of interatomic potentials and the state of stress. The paper is organized as follows. Section II contains details of the simulations. Section III contains the results of simulations and discussion. Section IV contains the concluding remarks.

II. SIMULATION DETAILS

Lennard-Jones type interaction potential of the form $V_{ij}=\alpha\left[\left(\frac{b}{r_{ij}}\right)^m-\left(\frac{b}{r_{ij}}\right)^6\right]$ is chosen for the simulation where V_{ij} is the pairwise interaction potential between the two atoms i and j; α, b, and m are potential parameters and r_{ij} is the separation distance between the two atoms i and j. Four different potentials are constructed by varying the exponent, m, of the repulsive term in the potential and keeping the curvature $\left[\frac{\partial^2 V_{ij}}{\partial r_{ij}^2}\right]_{r_0}$ of the potential and equilibrium separation distance, $r_0(=1.12b)$ as constants, so as to ensure that all the systems have similar atomic size and elastic stiffness values. These potentials are particular cases of the general Mie (m,n) potentials (see Ref. 13).

The parameters, calculated with the given constraints, are given in the Table I. The potential is truncated at R_{cut} $(=2.34b)$, which is chosen between fourth and fifth nearest neighbors, and smoothened by a cubic polynomial. The initial structure is built by generating a fcc lattice ($10\times10\times10$ unit cells, 4000 atoms) whose temperature is raised by incremental steps of 0.1 molecular dynamics (MD) units while maintaining zero pressure, starting from absolute zero, and a liquid state is obtained (melting temperature is between 2.5 and 3.5 MD units depending on the potential). During the

TABLE I. Values of potential parameters.

Potential	m	α	b	C_{11}[a]	C_{12}
I	8	14.22	0.97	127	72.5
II	12	4.00	1.00	103	56
III	16	2.16	1.01	95.3	52
IV	20	1.43	1.03	90.3	47

[a]All elastic constants are expresed in terms of reduced MD units.

simulations periodic boundary conditions are applied in all three directions. At each temperature the system is equilibriated for a time duration of 10 MD units. The radial distribution function, $g(r)$, is computed at each step to monitor structural changes. The liquid system thus formed is transformed to glass (at 0 K) by minimizing the total energy through a conjugate gradient algorithm. A characteristic split in the second peak of $g(r)$ is indicative of the short range order seen in glasses.[14] The glass, thus obtained, is subjected to a uniform deformation such that $\epsilon_{11}=\epsilon_h+\gamma/2$; $\epsilon_{22}=\epsilon_h-\gamma/2$; $\epsilon_{33}=\epsilon_h$, where ϵ_{11}, ϵ_{22}, and ϵ_{33} are the nonzero strain components (all other components are zero). The state of strain is chosen such that the sample is subjected to a shear strain γ (at 45° to the 1 and 2 axes) with a superimposed hydrostatic strain ϵ_h. Ten glass samples (different initial microstates) for each value of m are prepared and the following simulations are performed. (1) Shear strain, γ, is applied in increments of 0.1% up to $\gamma=50\%$ ($\epsilon_h=0$). (2) Hydrostatic strain, ϵ_h, is applied in increments of 0.1% up to $\epsilon_h=50\%$ ($\gamma=0$). (3) Hydrostatic strains of −3%, −1%, 1%, and 3% are superimposed on the shear strain, γ, which is increased up to 50% in increments of 0.1%. The sample is strained by incrementally scaling the periodic repeat distance of the simulation cell and the positions of the atoms appropriately. Care is taken so that opposite faces of the simulation cell do not come closer than $2R_{cut}$, where an atom interacts with its own image due to periodic boundary conditions.

III. RESULTS AND DISCUSSION

With the increase of the applied shear strain, the system undergoes deformations which have both elastic and inelastic components. Deformation proceeds by a build up of elastic energy which is released by local inelastic rearrangements of atoms which we call "plastic displacements" (see Fig. 1). In the initial part of deformation (at small applied shear strains) most of the atoms experience elastic displacements with very few plastic rearrangements. At larger strains, bursts of plastic rearrangements occur as shown in Fig. 1, with increase of strain, and are accompanied by a drastic drop of energy. Though the global shear strain is applied at 45° to the 1 and 2 axes, the displacement vectors are randomly oriented with a slight tendency to orient in the global shear direction. The direction of these displacements is governed largely by local environment seen by the atoms. The applied strain is, therefore, accommodated via a series of local rearrangements of atoms via "plastic displacements," with glass deforming elastically in the intermediate regions. At sufficiently large deformation simulations indicate deformation-induced crystallization as shown in Fig. 2. The crystalline phase formed due to the deformation is observed to be fcc with 111 planes parallel to shear axes, similar to the observations of Tarumi *et al.*,[7] who report MD simulations of pure shear deformation on Ni glass.

The shear strain at which the given glass transforms into crystalline configuration is termed as critical shear strain, γ_{cr}, and is taken as the parameter that reflects the intrinsic resistance of the given system to deformation-induced crystallization. At the onset of deformation-induced crystallization most of the atoms undergo plastic displacements and large scale rearrangements take place. In this process a few atoms cross a large potential energy barrier, E_b, of nearest neighboring atoms. The four types of glasses prepared essentially differ in their energy barrier, E_b, but have similar atomic sizes and stiffness values. The variation in the energy of an atom which passes through two adjoining atoms computed for the four types of glasses is shown in Fig. 3(a). A high value of m leads to a high E_b causing more resistance for the plastic displacements (when $m\rightarrow\infty$ the model corresponds to hard sphere model). A larger m effectively postpones the onset of crystallization and increases the γ_{cr}. The values of γ_{cr} for each of the glass samples vs E_b are shown in Fig. 3(b). The anticipated increasing trend of γ_{cr} with the E_b is clearly observed and provides important clues in understand-

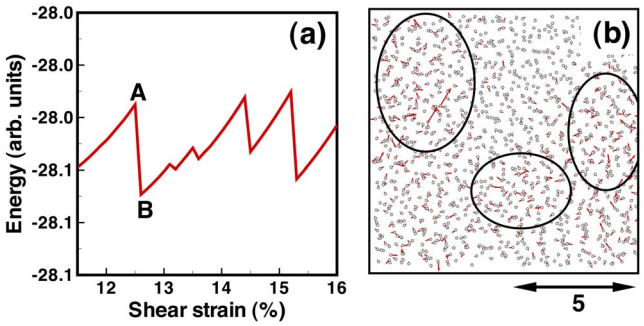

FIG. 1. (Color online) Left: Energy as a function of applied shear strain γ. The sudden decrease of energy is accompanied by local inelastic rearrangements of atoms (called "plastic displacements" in the text). Right: Vector plot of atomic plastic displacements during the deformation of a glass. The vectors shown, representing the plastic displacements, are relative positions of atoms in configuration B to those of A. The global shear strain is 45° to the 1 and 2 axes and $\epsilon_h=0$. The scale bar is shown in units of atomic diameters, and the displacement vectors are scaled in the same units of scale bar.

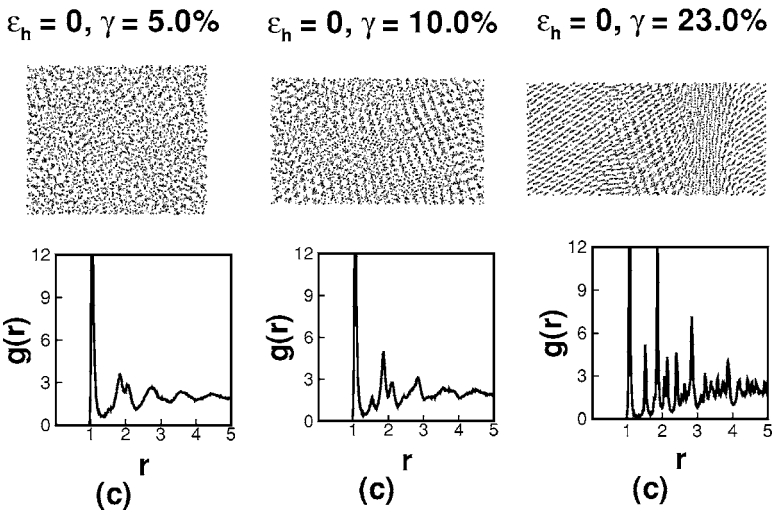

FIG. 2. An example of deformation-induced crystallization in a Lennard-Jones glass ($m=12$). (a) $\gamma=5.0\%$, (b) $\gamma=10.0\%$, and (c) $\gamma=23.0\%$. The crystallized phase is fcc.

ing the mechanisms for deformation-induced crystallization. The fraction of samples that crystallize during the deformation is also observed to decrease at high values of E_b or m. The critical shear strain γ_{cr} becomes insensitive to the value of E_b (or m) for larger values of m, the system fast approaches the "hard-sphere" limit. Lee *et al.*[6] studied the effect of "activation energy for crystallization" on plasticity of amorphous materials. They observed enhanced plasticity accompanied by crystallization with the decrease in activation energy. Our simulation results provide a direct observation of the above fact. The decrease in γ_{cr} with decrease in E_b indicate that glasses with low E_b are more ready to crystallize resulting in enhanced plasticity induced by crystallization. Lee *et al.*[6] also report that compressive stresses favor crystallization.

We now investigate the dependence of γ_{cr} on the superimposed hydrostatic strain ϵ_h. Figure 3(c) shows γ_{cr} plotted against ϵ_h for $m=12$ (simulation results are similar for other values of m). The critical strain, γ_{cr}, decreases at high compressive strains indicating enhanced possibility of deformation-induced crystallization at high hydrostatic pressures which is consistent with Lee *et al.*'s[6] experimental investigations. It is to be noted that though E_b increases with pressure, these results are consistent with the earlier interpretation of E_b dependence of γ_{cr}, since the dependence vanishes at high E_b values. The reduction of γ_{cr} is brought about by the stored elastic energy due to the hydrostatic compression, which now aids in the atoms to cross E_b. These results are in agreement with earlier reports of Aoki and Tsumaraya[15] who performed *ab initio* MD simulations on sodium glass and report enhanced deformation-induced crystallization at high pressures. They observed collapse of icosahedral clusters at high pressures enhancing the deformation-induced crystallization. We have performed simulations with pure hydrostatic strain (with $\gamma=0$). Neither plastic displacements of the atoms nor crystallization is observed in this case implying that a pure hydrostatic strain alone does not induce crystallization. However, experimental observations do indicate pressure-induced crystallization in semimetal systems like *a*-Se and *a*-Ge.[16,17] Though globally

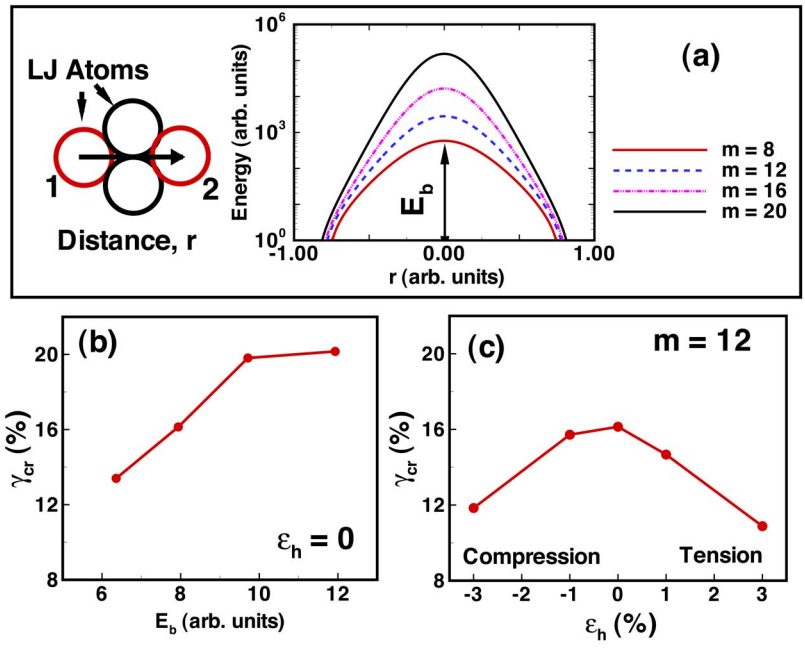

FIG. 3. (Color online) (a) The energy, E, of an atom along the path between two similar atoms just touching is plotted against the displacement from position 1 to 2. The barrier energy E_b is the maximum energy an atom needs to cross through atoms just touching each other. (b) The variation of critical shear strain γ_{cr} with energy barrier E_b. (c) The variation of critical shear strain γ_{cr} with superimposed hydrostatic strain ϵ_h.

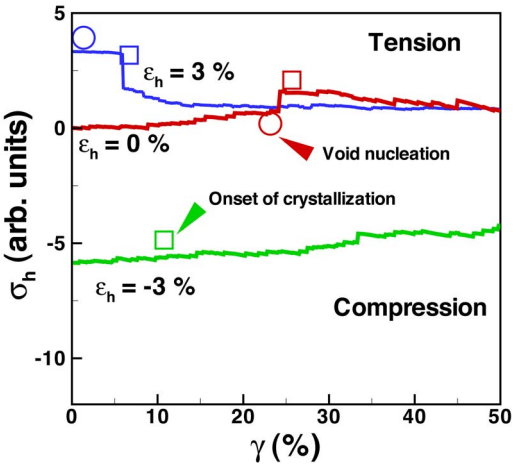

FIG. 4. (Color online) Variation of the hydrostatic stress, σ_h, with shear strain, γ, during the deformation process. Squares denote the onset of crystallization and circles denote the formation of voids. The upper curve represents the simulation performed with a positive hydrostatic strain. In this case voids are formed at the beginning of deformation. The second curve represents the simulation perfomed under zero hydrostatic strain. In this case voids are accompanied with crystallization. The third curve represents the simulation performed under compressive hydrostatic strain. Voids are absent in these simulations.

the stresses are purely hydrostatic in nature, the directional bonding in these systems may have resulted in non-close-packed structures and local shear stresses which in turn lead to crystallization. Since the interaction potentials we have used are spherically symmetric, anisotropy-induced shear stresses are absent in the system of present study.

Being disordered, (metallic) glasses tend to occupy higher volume than their corresponding close-packed crystallized states. In the present work, the simulated glasses have about 6% higher volume than the initial fcc configuration. Therefore the excess volume that is present due to deformation-induced crystallization can either lead to uniform distribution of vacancies in the crystal lattice or coalescence to form nano-voids. In our simulations, we have observed that nanocrystallization is associated with nano-void formation with nano-voids of the size of 4–6 atomic diameters. The variation of mean hydrostatic stress, σ_h, during the deformation process provides important clues to the mechanisms of void formation. In Fig. 4, simulations performed with three different values of hydrostatic strain are compared. Even though the global hydrostatic strain remains constant, we observe variations in the hydrostatic stress σ_h during the deformation, due to void formation and rearrangements of atoms. At the instant of void formation in the case of zero hydrostatic strain simulations, we observe a sudden rise in the σ_h. This is due to the fact that the simulation cell volume is kept constant while allowing for the reduction of the volume during crystal-to-glass transformation. In the case of simulations performed under tension, void formation occurs much earlier to crystallization and hence subsequent crystallization does not produce sudden increase in σ_h. On the contrary, crystallization and coalescence of voids leads to reduction of σ_h favoring reduction in the strain energy. The voids in the case

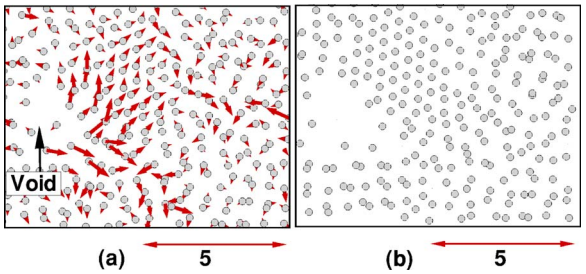

FIG. 5. (Color online) A slice of the simulation box showing a deformation induced void when ϵ_h=3%. High stress concentration near the void leads to high density of plastic rearrangements subsequently leading to crystallization. (a) and (b) are two succesive events during the deformation process. The scale bar is shown in units of atomic diameters. The displacement vectors are shown in the same units as scale bar.

of dilatational strains can lead to high stress concentrations favoring crystallization. From the vector plots of the atomic configuration (see, for example, Fig. 5) it is found that high density of atomic rearrangements occur near the void nucleating crystalline phases. This explains the decrease in γ_{cr}, in the tension part of Fig. 4(c). In the third case, compressive strain is applied such that the volume of the glass after compression is similar to that of initial crystalline configuration. Hence void formation is absent and an essentially constant σ_h is observed throughout the deformation process. These results are consistent with the transmission electron microscopy observations of bent metallic glass ribbon samples of Jiang and Atzmon,[4] who report the observation of nanocrystals on the compression side of the neutral axis and nanovoids on the tensile side.

We also monitored the volume occupied by an atom, Ω, through the deformation process. Here, Ω, is computed by making a Voronoi tessellation of the configuration and determining the volume of the Voronoi polyhedron corresponding to the given atom, which is computed by the Monte Carlo integration method. Figure 6 shows the atomic volume distributions of a glass sample (with m=12) at various stages of

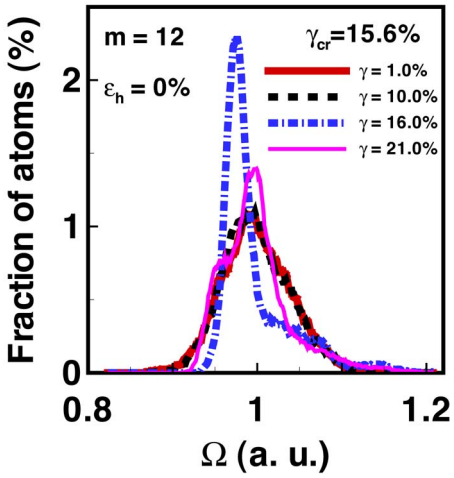

FIG. 6. (Color online) Atomic volume distributions during the various stages of deformation for an LJ glass at ϵ_h=0.

its deformation. The spread in the atomic volumes is wider for amorphous structure compared to crystalline structures. The distribution is maintained without any gross changes until the onset of crystallization. After the onset of crystallization the distribution narrows dramatically indicating a drastic reduction in free volume. Continued deformation also results in partial reamorphization of the crystalline structures and further recrystallization. These rearrangements provide a micromechanism for dissipation of energy in continued plastic deformation.

IV. CONCLUSIONS

Our study uncovers several key points pertaining to the mechanisms of plastic accommodation in glasses, such as crystallization and void formation. The propensity of a glass to undergo crystallization upon deformation is strongly governed by the short range repulsive potential; glasses made up of atoms with softer short range potentials will show increased tendency for deformation-induced crystallization. A compressive hydrostatic strain aids crystallization while a tensile hydrostatic strain induces voids. Further, a state of shear is found essential to induce crystallization. Our analysis indicates that there is a net free volume reduction upon crystallization. Deformation subsequent to crystallization leads to partial reamorphization and recrystallization, suggesting an important micromechanism for plastic dissipation. While real glasses have more than one component with different bonding characteristics, our study of a single component system provides a simple picture of the factors affecting the micromechanisms of strain accommodation during inelastic deformation of glasses.

ACKNOWLEDGMENTS

P.M. gratefully acknowledges useful and insightful discussion with S. Ranganathan and R. Raghavan. The authors acknowledge support for this work by DMRL Hyderabad.

*Email address: shenoy@mrc.iisc.ernet.in

[1] H. Chen, Y. He, G. J. Shiflet, and S. J. Poon, Nature (London) **367**, 541 (1994).
[2] J. J. Kim, Y. Choi, S. Suresh, and A. S. Argon, Science **295**, 654 (2002).
[3] J. Li, Z. L. Wang, and T. C. Hufnagel, Phys. Rev. B **65**, 144201 (2002).
[4] W. H. Jiang and M. Atzmon, Acta Mater. **51**, 4095 (2003).
[5] R. Bhowmick, R. Raghavan, K. Chattopadhyay, and U. Ramamurty, Acta Mater. **54**, 4221 (2006).
[6] S. W. Lee, M. Y. Huh, E. Fleury, and J. C. Lee, Acta Mater. **54**, 349 (2006).
[7] R. Tarumi, A. Ogura, M. Shimojo, K. Takashima, and Y. Higo, Jpn. J. Appl. Phys., Part 2 **39**, L611 (2000).
[8] B. J. Lee, C. S. Lee, and J. C. Lee, Acta Mater. **51**, 6233 (2003).
[9] W. J. Wright, R. Saha, and W. D. Nix, Mater. Trans., JIM **42**, 642 (2001).
[10] Z. F. Zhang, J. Eckert, and L. Schultz, Acta Mater. **51**, 1167 (2003).
[11] R. Vaidyanathan, M. Dao, G. Ravichandran, and S. Suresh, Acta Mater. **49**, 3781 (2001).
[12] C. A. Schuh and A. C. Lund, Nat. Mater. **2**, 449 (2003).
[13] W. Brostow, *Science of Materials* (Wiley, New York, 1979).
[14] M. Tsumaraya and M. S. Watanabe, J. Chem. Phys. **92**, 4983 (1990).
[15] M. I. Aoki and K. Tsumaraya, Phys. Rev. B **56**, 2962 (1997).
[16] K. Tanaka, Phys. Rev. B **42**, 11245 (1990).
[17] K. Tanaka, Phys. Rev. B **43**, 4302 (1991).